set of calculated data have been filed with the ACS Microfilm Depository Service.

Nomemclature

G^E = excess Gibbs free energy, cal/g-mol

x_1 = mole fraction of the more volatile component of a binary mixture in the liquid phase

y_1 = mole fraction of the more volatile component of a binary mixture in the vapor phase

γ_1, γ_2 = activity coefficients for components 1 and 2 in the liquid phase

ϕ_1, ϕ_2 = coefficient of correction for nonideality of the vapor phase for components 1 and 2

π = total pressure, mm Hg

Literature Cited

(1) Minh, D. C., MS thesis, Sherbrooke University, Sherbrooke, Que., Canada (1970).
(2) Minh, D. C., Ruel, M., *Can. J. Chem. Eng.*, **48**, 501 (1970).
(3) Minh, D. C., Ruel, M., *ibid.*, **49**, 159 (1971).
(4) Prengle, H. W., Palm, G. F., *Ind. Eng. Chem.*, **49**, 1769 (1957).
(5) Ramalho, R., Delmas, J., *Can. J. Chem. Eng.*, **46**, 32 (1968).
(6) Ramalho, R., Delmas, J., *J. Chem. Eng. Data*, **13**, 161 (1968).
(7) Selected Values of Properties of Chemical Compounds. Thermodynamics Research Center, Texas A&M University, College Station, Tex., 1970.

Received for review January 19, 1971. Resubmitted February 10, 1972. Accepted October 26, 1972. Grants from the National Research Council of Canada are gratefully acknowledged. Additional data will appear following these pages in the microfilm edition of this volume of the Journal. Single copies may be obtained from the Business Operations Office, Books and Journals Division, American Chemical Society, 1155 Sixteenth St., N.W., Washington, D.C. 20036. Refer to the following code number: JCED-73-41. Remit by check or money order $7.00 for photocopy or $2.00 for microfiche.

Vapor-Liquid Equilibria in Mixtures of Water, *n*-Propanol, and *n*-Butanol

Richard A. Dawe,[1] **David M. T. Newsham,**[2] **and Soon Bee Ng**
Department of Chemical Engineering, University of Manchester Institute of Science and Technology, Manchester, M60 1QD, U.K.

Measurements of vapor-liquid equilibria in the systems water-*n*-propanol and water-*n*-propanol-*n*-butanol at atmospheric pressure are reported. The results for the ternary system have been compared with those predicted from the binary mixtures using the equation of Renon and Prausnitz. Agreement is very satisfactory. Densities and refractive indices of the binary and ternary mixtures at 25°C are also reported and the excess volumes of binary mixing have been calculated.

This paper reports the results of measurements of vapor-liquid equilibria for the systems water-*n*-propanol and water-*n*-propanol-*n*-butanol at atmospheric pressure. Enthalpies of mixing for these systems have previously been reported (*5, 6*) and liquid-liquid equilibrium studies have also been published (*10*).

Vapor-liquid equilibria in the system water-*n*-propanol have been extensively investigated (*7*) and this system is therefore suitable for testing the performance of the equilibrium still used in the present work. No measurements of vapor-liquid equilibria in the system water-*n*-propanol-*n*-butanol have previously been reported.

Experimental

Materials used in this investigation were purified as described in ref. *5* and *6*.

For the measurements of vapor-liquid equilibria, an equilibrium flow still similar to that described by Vilim et al. (*14*) was constructed. This instrument has the advantage that it avoids recirculation of the condensed vapor, which enables reasonably precise results to be obtained in a short time (15 min). The still used in this work differed from that of Vilim et al. in that the thermometer well was designed to accommodate a 50-ohm capsule-type platinum resistance thermometer (Rosemount Engineering Co. Ltd.) and the vacuum jacket that insulated the equilibrium chamber was extended to include the droplet separator (Figure 1) in order to minimize thermal

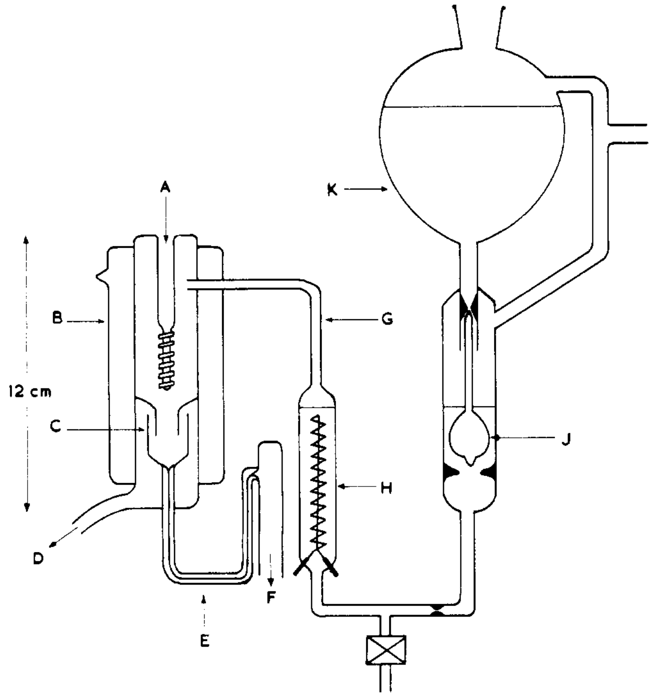

Figure 1. Equilibrium chamber of the flow still
A, thermometer well; B, vacuum jacket; C, droplet separator; D, to vapor condenser; E, 3-mm capillary; F, to liquid cooler; G, Cottrell pump; H, boiler; J, float-valve; *K*, reservoir

---

[1] Present address, Department of Chemical Engineering, University of Leeds, Leeds, U.K.

[2] To whom correspondence should be addressed.

losses. The platinum thermometer was calibrated by intercomparison with a 25-ohm platinum thermometer that had been calibrated at the National Physical Laboratory (U.K.) on the International Practical Temperature Scale of 1948. Resistances were measured by potentiometric comparison with a 100-ohm standard resistor on a vernier potentiometer (H. Tinsley and Co. Ltd., U.K.). Temperatures could be measured to within ±0.02°C with the platinum thermometer. No attempt was made to control the pressure in the equilibrium still, but the pressure in the laboratory was measured by a mercury manometer and cathetometer with an accuracy of ±0.05 mm Hg. All pressures were corrected to give the equivalent height of a mercury column at 0°C and standard gravity. For this purpose a value of the local acceleration due to gravity of 981.370 ± 0.001 cm sec^{-2} was used.

Preliminary measurements in which pure water was boiled in the still showed that thermal equilibrium could be attained in it to within 0.02°C. Subsequent experiments with water and *n*-propanol mixtures indicated also that transfer of material between vapor and liquid phases was sufficiently rapid for a reasonable approach to equilibrium conditions to be made. The ratio of liquid to vapor flow rates was, typically, about 10. The droplet separator functioned satisfactorily throughout the measurements and no indications of entrainment in either vapor or liquid phases were observed. The liquid samples were always used in the freshly distilled state since they were continually recycled through the still.

Compositions of the binary liquid mixtures were determined by measurement of their refractive indices, and those of the ternary mixtures were deduced from density and refractive index measurements. A dipping refractometer that was equipped with thermoprisms (Carl Zeiss, Jena) and which had a measuring precision of $\pm 2 \times 10^{-5}$ was used. The temperature of the prisms was controlled at 25.00° ± 0.05°C by circulating water from a thermostat. Illumination was provided by a sodium lamp. Densities were measured at 25°C using 5-cm^3 Lipkin pycnometers that had been calibrated with distilled water. The density of water at 25°C was taken to be 0.99705 gram cm^{-3}. The precision of the density measurements was estimated to be ±0.0002 gram cm^{-3}. Calibration curves for composition as a function of density and refractive index were prepared by measuring these properties for samples of known composition. For estimating ternary compositions it was necessary to prepare curves of constant density and refractive index as a function of composition. This was achieved by interpolating the primary results graphically to give the curves of Figure 2.

The estimated errors in the measured mole fractions are different for each component. They are ±0.005 for water and ±0.01–0.05 for *n*-propanol and *n*-butanol. The reason for this is apparent on examination of Figure 2 which shows that the curves of constant density are almost vertical straight lines. This means that the percentage of water (W_1) can always be accurately estimated because it is virtually independent of the angle at which the curves of constant density and refractive index intersect. The percentage of propanol (W_2) is more difficult to determine particularly in the region $40 < W_1 < 60\%$ where the density and refractive index curves are almost parallel to each other. The butanol composition (W_3) is also subject to considerable uncertainty in this region. For values of $W_1 < 40\%$, however, W_1 and W_3 can be determined to within about 1%. These estimates of the uncertainties are substantiated in the comparison of experimental and calculated vapor compositions made later.

Results and Discussion

The densities and refractive indices for the three binary systems and the ternary system at 25°C are recorded in Table I. Table II gives densities and refractive indices measured at 25.9°C for mixtures with compositions lying on the liquid-liquid phase boundary at 25°C.

The excess volumes of mixing for the three binary systems have been computed from the densities and are recorded in Figure 3. The vertical error bars for the *n*-propanol–*n*-butanol system represent an uncertainty in the density measurements of ±0.0002 gram cm^{-3}. The apparent asymmetry is probably not real. The other excess thermodynamic functions are not asymmetric (*6*).

Vapor-liquid equilibrium results for the systems water–*n*-propanol and water–*n*-propanol–*n*-butanol are presented in Tables III and IV, respectively. References to vapor-liquid equilibrium data for water–*n*-propanol may be

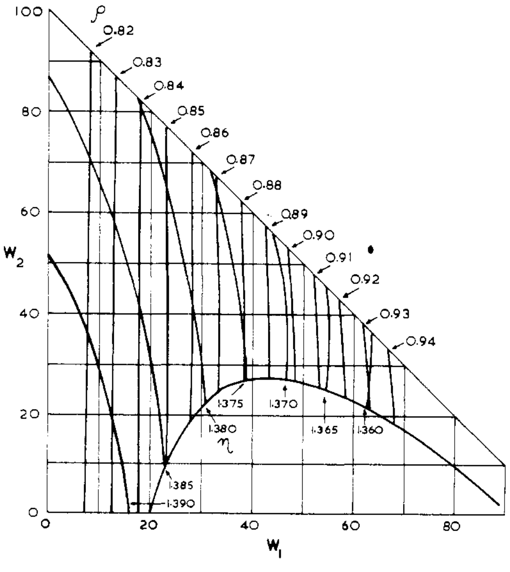

Figure 2. Curves of constant density and refractive index for water (1)–*n*-propanol (2)–*n*-butanol (3) at 25°C

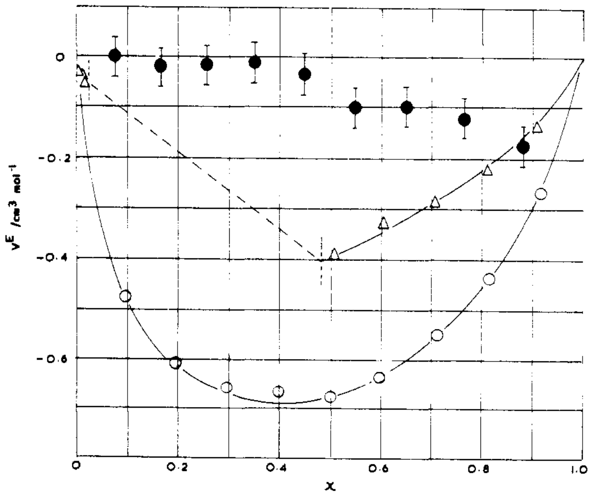

Figure 3. Excess volumes of mixing of water–*n*-propanol (○), water–*n*-butanol (△), and *n*-propanol–*n*-butanol (●) at 25°C; *x* is the mole fraction of the second component

Table I. Densities and Refractive Indices of Solutions of Water, *n*-Propanol, and *n*-Butanol at 25°C

W_1	W_2	W_3	ρ/gram cm^{-3}	η
100	0	0	0.99705	1.33252
0	100	0	0.80034	1.38325
0	0	100	0.80594	1.39727
2.51	97.49	0	0.80737	1.38311
6.31	93.69	0	0.81599	1.38264
10.75	89.25	0	0.82537	1.38182
16.51	83.49	0	0.83743	1.38022
22.69	77.31	0	0.85012	1.37835
30.96	69.04	0	0.86652	1.37533
41.08	58.92	0	0.88751	1.37119
55.05	44.95	0	0.91688	1.36460
72.93	27.07	0	0.95394	1.35466
0	90.84	9.16	0.80081	1.38446
0	80.38	19.62	0.80163	1.38596
0	70.10	29.90	0.80217	1.38741
0	59.99	40.01	0.80266	1.38883
0	49.64	50.36	0.80347	1.39024
0	39.84	60.16	0.80464	1.39158
0	30.29	69.71	0.80514	1.39293
0	19.90	80.10	0.80590	1.39442
0	9.64	90.36	0.80696	1.39573
2.32	0	97.68	0.81084	1.39683
5.27	0	94.73	0.81657	1.39581
9.06	0	90.94	0.82368	1.39429
13.55	0	86.45	0.83202	1.39227
18.89	0	81.11	0.84211	1.38959
93.85	0	6.15	0.98788	1.33851
94.64	0	5.36	0.98903	1.33782
96.96	0	3.04	0.99210	1.33539
98.37	0	1.63	0.99443	1.33405
5.5	84.4	10.1	0.81373	1.38424
7.2	21.9	70.9	0.81933	1.39216
7.4	41.0	51.6	0.81906	1.38950
7.4	51.9	40.7	0.81886	1.38801
7.4	89.3	3.3	0.81780	1.38300
7.9	71.5	20.6	0.81914	1.38517
9.0	7.6	83.4	0.82309	1.39342
9.9	29.9	60.2	0.82447	1.39004
15.2	12.6	72.2	0.83496	1.38995
17.1	74.0	8.9	0.83959	1.38129
19.4	58.1	22.5	0.84291	1.38225
20.3	44.6	35.1	0.84422	1.38352
22.5	25.9	51.6	0.84881	1.38476
29.2	37.0	33.8	0.86167	1.38000
31.1	49.5	19.4	0.86586	1.37758
33.0	59.8	7.2	0.87023	1.37546
42.9	35.6	21.5	0.88883	1.37251
45.6	36.5	17.8	0.89464	1.37090
57.9	30.1	12.0	0.91975	1.36398
60.0	35.9	4.1	0.92556	1.36230
77.8	19.5	2.7	0.96196	1.35149

Table II. Refractive Indices and Densities of Mixtures of Water, *n*-Propanol, and *n*-Butanol at 25.9°C and at Compositions Lying on the Binodal Curve at 25°C

W_1	W_2	η	ρ/g cm^{-3}
21.6	7.7	1.38609	0.84643
31.4	23.4	1.37931	0.86490
40.5	27.2	1.37395	. . .
55.6	25.2	1.36465	. . .
72.5	16.4	1.35290	. . .
77.8	13.6	1.35085	0.95925
80.8	11.9	1.34870	0.96558

Table III. Vapor-Liquid Equilibrium Data for Water (1)–*n*-Propanol (2)

P, mm Hg	t, °C	x_2	y_2	γ_1	γ_2
756.33	98.18	0.0031	0.071	0.989	21.8
756.73	96.47	0.0068	0.131	0.988	19.6
756.73	93.91	0.0130	0.215	0.985	18.5
756.73	91.92	0.0218	0.288	0.970	15.9
756.07	88.57	0.072	0.375	1.015	7.126
755.86	88.04	0.139	0.393	1.083	3.948
757.97	87.72	0.275	0.407	1.276	2.098
757.97	87.62	0.327	0.415	1.361	1.806
757.97	87.54	0.380	0.424	1.459	1.593
758.08	87.53	0.396	0.421	1.507	1.519
758.08	87.62	0.515	0.456	1.756	1.260
758.08	88.97	0.721	0.561	2.344	1.051
756.33	89.40	0.766	0.596	2.525	1.032
759.13	91.69	0.867	0.710	2.939	0.998
759.13	93.07	0.913	0.785	3.166	0.994
759.13	94.87	0.955	0.878	3.252	0.994

found in the compilation of Hala et al. (*7*). For the purpose of evaluating the performance of the equilibrium still used in the present investigation we have compared the data selected by Hala et al. (*8*) with our results in Figure 4 which is a plot of vapor phase composition against liquid phase composition. The average deviation of the vapor compositions determined in this work from the smooth curve of Figure 4 is 0.001. We find, for the azeotropic composition, $y_2 = x_2 = 0.433$ compared to values of 0.432 and 0.426 given by Doroshevsky and Polansky (*3*) and Murti and Van Winkle (*9*). At other compositions the agreement is generally good; the largest deviations (up to 0.04) occur at low alcohol concentrations where difficulties are encountered in operating an equilibrium still because of the rapid change of boiling point with composition in this region. The boiling points of pure water and *n*-propanol obtained by extrapolation of the $t - x$ diagram, after correction to 760 mm Hg, were 100.03° and 97.13°C compared to values of 100.00° and 97.07°C calculated from the Antoine equations of ref. *8*. The estimated error on the extrapolated values of the boiling points is 0.1°C.

The validity of the results may also be checked by applying thermodynamic consistency tests to the liquid phase activity coefficients. The latter were calculated from the following equation which includes corrections for vapor phase nonideality:

$$\gamma_i = (y_i P / x_i P_i^{\circ}) \exp\left[(B_{ii} - V_L)(P - P_i^{\circ})/RT\right] \tag{1}$$

This equation assumes that the vapor phase behaves as an ideal solution. The reference state for the activity coefficients is the pure liquid at the temperature and total pressure of the solution. The second virial coefficients for water and *n*-propanol were taken from the work of Collins and Keyes (*1*) and Cox (*2*), respectively, and the pure component vapor pressures were calculated from the Antoine equations given in ref. *8*. The maximum value of the vapor phase correction was 1.5%. The consistency test was applied by writing the Gibbs-Duhem equation in the form

$$\int_{x_1=0}^{x_1=1} \ln(\gamma_1/\gamma_2)dx_1 - \int_{x_1=0}^{x_1=1} \frac{H^E}{RT^2}\left(\frac{\partial T}{\partial x_1}\right)_P dx_1 = 0 \tag{2}$$

Figure 5 is a plot of $\ln \gamma_1/\gamma_2$ against x_1. The area ratio $|A_1/A_2|$ obtained by Simpson's rule integration is 0.975.

Table IV. Vapor-Liquid Equilibrium Data for Water (1) and *n*-Propanol (2)–*n*-Butanol (3)

				Exptl		Calcd Eq 7				
P, mm Hg	t, °C	x_1	x_2	y_1	y_2	y_1	y_2	Δy_1	Δy_2	Δy_3
760.58	100.21	0.141	0.197	0.432	0.170	0.439	0.216	−0.007	−0.046	+0.053
760.56	96.37	0.153	0.409	0.382	0.421	0.398	0.408	−0.016	+0.013	+0.003
760.47	94.88	0.155	0.517	0.367	0.492	0.371	0.489	−0.004	+0.003	+0.001
760.56	93.44	0.166	0.611	0.352	0.571	0.362	0.547	−0.010	+0.024	−0.014
760.64	92.20	0.168	0.697	0.344	0.615	0.348	0.604	−0.004	+0.011	−0.007
765.92	91.73	0.176	0.748	0.354	0.618	0.345	0.623	+0.009	−0.005	−0.004
761.67	91.82	0.372	0.233	0.602	0.247	0.613	0.207	−0.011	+0.040	−0.029
761.84	92.76	0.374	0.144	0.633	0.142	0.646	0.133	−0.013	+0.009	+0.004
762.90	90.22	0.377	0.503	0.542	0.401	0.530	0.422	+0.012	−0.021	+0.009
765.71	88.73	0.406	0.539	0.535	0.436	0.528	0.454	+0.007	−0.018	+0.011
765.68	90.06	0.490	0.303	0.616	0.286	0.622	0.279	−0.006	+0.009	−0.003
762.92	88.87	0.572	0.338	0.607	0.338	0.609	0.343	−0.002	−0.005	+0.007
761.84	89.93	0.589	0.226	0.649	0.243	0.660	0.235	−0.011	+0.008	+0.003
765.72	89.74	0.623	0.239	0.646	0.261	0.651	0.265	−0.005	−0.004	+0.009
765.59	88.43	0.689	0.307	0.607	0.359	0.591	0.405	+0.016	−0.046	+0.030
762.56	89.27	0.749	0.210	0.639	0.307	0.630	0.330	+0.009	−0.023	+0.014
765.47	88.91	0.857	0.129	0.635	0.318	0.625	0.340	+0.010	−0.022	+0.012
							Average	0.009	0.019	0.013

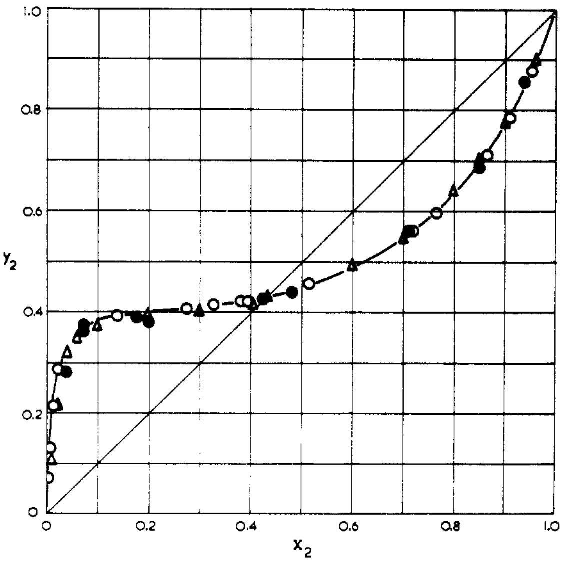

Figure 4. Equilibrium vapor and liquid compositions for water–*n*-propanol at atmospheric pressure
○ this work, △ Doroshevsky and Polansky (3), ● Murti and Van Winkle (9).

This is satisfactory since the second term of Equation 2 has been neglected. However, this integral may be evaluated using the enthalpies of mixing of Plewes et al. (*11*) and from values of $(\partial T/\partial x_1)_P$ obtained by graphical differentiation of the $t - x$ curve. When this is done the area ratio is increased to a value of 0.995. The corrected curve cannot be shown with clarity in Figure 5 but the main differences occur for values of $x_1 < 0.2$ and > 0.9 because of the high values of $(\partial T/\partial x_1)_P$ in these regions. The closeness of the area ratio to unity confirms the thermodynamic consistency of our results.

Figure 5 also indicates the high precision of the results for the water–*n*-propanol system, as does Figure 6 which is a plot of the excess Gibbs energy against x_2.

The results of the measurements on the ternary system are collected together in Table IV, and are discussed below.

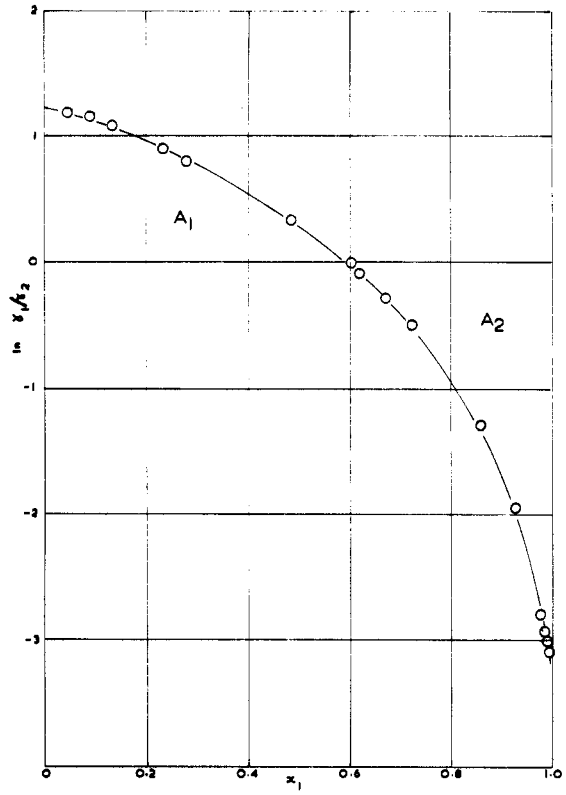

Figure 5. Plot of ln (γ_1/γ_2) against x_1 for water (1)–*n*-propanol (2) at atmospheric pressure

Prediction of Ternary Phase Equilibria

Recently, Renon and Prausnitz (*12*) have proposed a method of evaluating the thermodynamic properties of multicomponent mixtures from a knowledge only of the properties of the appropriate binary pairs. The method is particularly suitable for partially miscible systems. We have therefore applied it to the system water–*n*-propanol–*n*-butanol. According to Renon and Prausnitz the excess Gibbs free energy of a binary liquid mixture is given by the following Equation:

$$G^E/RT = x_1x_2\left[\tau_{21}G_{21}/(x_1 + x_2G_{21}) + \tau_{12}G_{12}/(x_2 + x_1G_{12})\right] \quad (3)$$

Table V. Parameters of the Equation of Renon and Prausnitz for Binary Systems of Water (1), *n*-Propanol (2), and *n*-Butanol (3)

$(g_{21} - g_{11})/R = 77.33K$	$(g_{12} - g_{22})/R = 865.41K$	$\alpha_{12} = 0.3772$
$(g_{32} - g_{22})/R = 3.80K$	$(g_{23} - g_{33})/R = 3.80K$	$\alpha_{23} = 0$
$(g_{13} - g_{33})/R = 1596.63K$	$(g_{31} - g_{11})/R = 331.13K$	$\alpha_{31} = 0.4240$

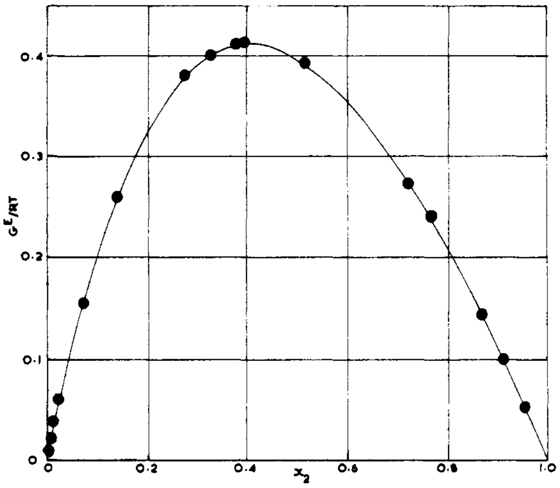

Figure 6. Plot of the excess Gibbs free energy against x_2 for water (1)-*n*-propanol (2) at atmospheric pressure

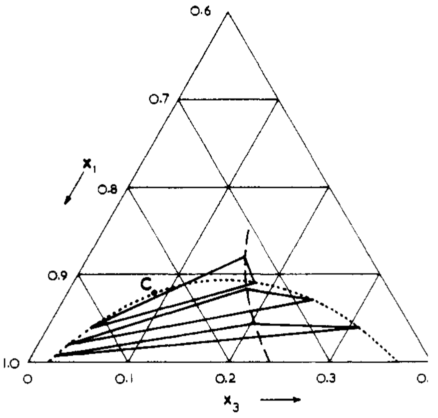

Figure 7. Projection of the phase diagram for water-*n*-propanol-*n*-butanol at 760 mm Hg
-- vapor 3-phase curve, ···· liquid 3-phase curves, ——— tie triangles, C critical point

where $\tau_{21} = (g_{21} - g_{11})/RT$, $\tau_{12} = (g_{12} - g_{22})/RT$, $G_{21} = \exp(-\alpha_{21}\tau_{21})$, $G_{12} = \exp(-\alpha_{12}\tau_{12})$, and $\alpha_{12} = \alpha_{21}$.

The quantities g_{ij} are interaction energies and α_{12} is the so-called "nonrandomness parameter." The three independent parameters of Equation 3 were obtained for the three binary systems by making a nonlinear least-squares fit to the excess Gibbs energies, assuming the parameters to be independent of temperature. The data for *n*-propanol-*n*-butanol and water-*n*-butanol were those of Gay (*4*) and Smith and Bonner (*13*), respectively. The excess Gibbs energies for the system *n*-propanol-*n*-butanol are much smaller than those of the other two systems and, within the experimental error, G^E is a symmetrical function of composition. For this system, therefore, the parameter α_{ij} was taken to be zero when Equation 3 reduces to the second-order Margules equation:

$$G^E = 2x_1x_2(g_{21} - g_{11}) \tag{4}$$

The binary parameters are given in Table V. All of the systems could be fitted to Equation 3 with root-mean-square deviations of less than 0.003 in G^E/RT.

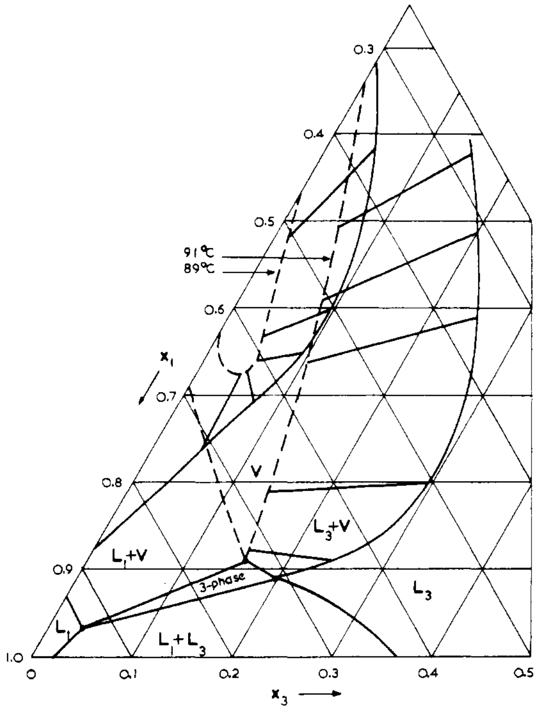

Figure 8. Isothermal sections (with tie-lines) of the phase diagram for water-*n*-propanol-*n*-butanol at 89° and 91°C
-- vapor curves, ——— liquid curves

The binary parameters were then used in Equation 5, which is the ternary form of the Renon-Prausnitz equation, to calculate the activity coefficients of the ternary system and hence bubble point temperatures and vapor phase compositions at 760 mm Hg:

$$\ln\gamma_i = \frac{\sum_{j=1}^{3}\tau_{ji}G_{ji}x_j}{\sum_{l=1}^{3}G_{li}x_l} + \sum_{j=1}^{3}\frac{x_jG_{ij}}{\left(\sum_{l=1}^{3}G_{lj}x_l\right)}\left[\tau_{ij} - \frac{\left(\sum_{r=1}^{3}x_r\tau_{rj}G_{rj}\right)}{\left(\sum_{l=1}^{3}G_{lj}x_l\right)}\right] \tag{5}$$

where $G_{kk} = 1$ and $\tau_{kk} = 0$.

The results of the calculations are given in Table IV where the vapor phase compositions are compared with the experimental values. The agreement is very satisfactory, bearing in mind the limitations of the analytical method used for obtaining the compositions of *n*-propanol and *n*-butanol.

Equation 5 has also been used to examine the phase diagram in the vicinity of the liquid-liquid region. In an attempt to establish the liquid-liquid phase boundary and tie-lines by searching (graphically) for the compositions at which the activities of each component were uniform, it was found that the equilibrium compositions were too sensitive to small changes in the activity for a reliable estimate of the binodal curve to be made. Instead, estimates of the binodal curves at temperatures close to the bubble point were made by extrapolating the liquid-liquid equilibrium data previously reported (*10*). Liquid-liquid tie-lines were then obtained by finding the compositions at which curves of constant activity of *n*-propanol intersected the binodal curve. The resultant liquid and vapor three-phase curves are shown, in projection, in Figure 7. The three-phase curves cover a range of boiling points of only about 3°C.

The system does not form a ternary azeotrope, homogeneous or heterogeneous. The vapor and liquid surfaces are rather flat, however, in the region between the homogeneous water–propanol azeotrope and the heterogeneous water–butanol azeotrope. This is evident on inspection of two isothermal sections of the phase diagram at 89° and 91°C, as shown in Figure 8.

Acknowledgment

We are grateful to G. L. Standart for his encouragement. We are also indebted to F. P. Stainthorp and H. M. Rash for their guidance in the preparation of the necessary computer programs.

Nomenclature

B_{ij} = second virial coefficient, $cm^3 mol^{-1}$
G^E = excess Gibbs free energy of mixing, $J mol^{-1}$
G_{ij} = parameter of Renon-Prausnitz equation
g_{ij} = parameter of Renon-Prausnitz equation
H^E = excess enthalpy of mixing, $J mol^{-1}$
P = total pressure, mm Hg
P_i^o = pure component vapor pressure, mm Hg
R = gas constant, $J K^{-1} mol^{-1}$
T = Kelvin temperature, K
t = Celsius temperature, °C
V^E = excess volume of mixing, $cm^3 mol^{-1}$
W_i = wt %
x_i = liquid phase mole fraction
y_i = vapor phase mole fraction

Greek Letters

α_{ij} = parameter of Renon-Prausnitz equation
γ_i = liquid phase activity coefficient
η = refractive index (sodium D-line)
ρ = density, $g cm^{-3}$
τ_{ij} = parameter of Renon-Prausnitz equation

Subscripts

1 = water
2 = *n*-propanol
3 = *n*-butanol
i,j,k,l,r = running variables

Literature Cited

(1) Collins, S. C., Keyes, F. G., *Proc. Amer. Acad. Sci.*, **72**, 283 (1938).
(2) Cox, J. D., *Trans. Faraday Soc.*, **57**, 1674 (1961).
(3) Doroshevsky, A., Polansky, E., *Z. Phys. Chem.*, **73**, 192 (1910).
(4) Gay, L., *Chim. Ind.* **18**, 187 (1927).
(5) Goodwin, S. R., Newsham, D. M. T., *J. Chem. Thermodyn.*, **3**, 325 (1971).
(6) Goodwin, S. R., Newsham, D. M. T., *ibid.*, **4**, 31 (1972).
(7) Hala, E., Pick, J., Fried, V., Vilim, O., "Vapour-Liquid Equilibrium," 2nd ed., p 404, Pergamon, London, 1967.
(8) Hala, E., Wichterle, I., Polák, J., Boublik, T., "Vapour-Liquid Equilibrium Data at Normal Pressures," Pergamon, London, 1968.
(9) Murti, P. S., Van Winkle, M., *Ind. Eng. Chem.*, **3**, 72 (1958).
(10) Newsham, D. M. T., Ng, S. B., *J. Chem. Eng. Data*, **17** (2), 205 (1972).
(11) Plewes, A. C., Jardine, D. A., Butler, R. M., *Can. J. Technol.*, **32**, 133 (1954).
(12) Renon, H., Prausnitz, J. M., *AIChE J.*, **14**, 135 (1968).
(13) Smith, T. E., Bonner, R. F., *Ind. Eng. Chem.*, **41**, 2867 (1949).
(14) Vilim, O., Hala, E., Pick, J., Fried, V., *Collect. Czech. Chem. Commun.*, **19**, 1330 (1954).

Received for review March 30, 1972. Accepted August 21, 1972. S. B. Ng received financial support from the British Council.

Integral Isobaric Heat of Vaporization of Benzene-1,2-Dichloroethane System

Yaddanapudi Jagannadha Rao and Dabir S. Viswanath[1]
Department of Chemical Engineering, Indian Institute of Science, Bangalore-12, India

Integral isobaric heats of vaporization of benzene-1,2-dichloroethane mixtures were measured at pressures of 684 and 760 mm of Hg using a modified Dana's apparatus. The results were found to be linear with composition.

Latent heat of vaporization is a very important property needed in the design and operation of chemical plants. Several investigators have therefore devised methods for the determination of this property. Very little data (*1, 2, 6–10, 12, 13, 15*) are available on heat of vaporization of mixtures.

The first published work on latent heats of mixtures was by Dana (*2*) who worked at atmospheric pressure and cryogenic temperatures. Apart from other sources of error, the main source of error in his experimentation was due to heat leak because of the considerable temperature gradient between the system and the surroundings. Subsequently, attempts have been made (*6–10, 12, 13*) to minimize the heat leak and reduce other sources of error involved. The best modification was due to Shettigar et al. (*9*) who introduced a liquid meter also to avoid changes in the equilibrium condition of the experiment.

Experimental

Materials. Benzene used was of Pro analysi grade produced by Sarabhai Merck Ltd., India, with a reported boiling range of 80–81°C. This material was subjected to the thiophene test. Thiophene was removed by treating it with concentrated sulfuric acid and distilling it after separation and washing it with distilled water. Benzene then was dried over calcium chloride, filtered, and further purified in a distillation column. Only the middle fractions of the distillate were collected. Table I gives a comparison of the experimentally determined physical properties with the literature values.

---

[1] To whom correspondence should be addressed.